

2023

Shear Capacity of Fiber Reinforced Concrete (FRC) Beams with Openings Strengthened using various systems and materials

Hind Mohamed, A. H. Abdel-Kareem, Mohamed H. Makhlof

Follow this and additional works at: <https://digitalcommons.aaru.edu.jo/erjeng>

Recommended Citation

Mohamed, A. H. Abdel-Kareem, Mohamed H. Makhlof, Hind (2023) "Shear Capacity of Fiber Reinforced Concrete (FRC) Beams with Openings Strengthened using various systems and materials," *Journal of Engineering Research*: Vol. 7: Iss. 3, Article 6.

Available at: <https://digitalcommons.aaru.edu.jo/erjeng/vol7/iss3/6>

This Article is brought to you for free and open access by Arab Journals Platform. It has been accepted for inclusion in Journal of Engineering Research by an authorized editor. The journal is hosted on [Digital Commons](#), an Elsevier platform. For more information, please contact rakan@aar.edu.jo, marah@aar.edu.jo, u.murad@aar.edu.jo.



Shear Capacity of Fiber Reinforced Concrete (FRC) Beams with Openings Strengthened Using Various Systems and Materials

A.H. Abdel-Kareem¹, H.H Mohamed², M.H. Makhlof³

¹ Professor, Department of Civil Engineering, Benha Faculty of Engineering, Benha University, Egypt- email: ahmed.abdelkareem@bhit.bu.edu.eg

² MSC. Student, Department of Civil Engineering, Benha Faculty of Engineering, Benha University, Egypt- email: hend.mansour18@bhit.bu.edu.eg

³ Associated Professor, Department of Civil Engineering, Benha Faculty of Engineering, Benha University, Egypt- email: mohamedmakhlof83@yahoo.com

Abstract- This study presents the findings of an experiment conducted on eleven identical fiber-reinforced concrete beams with two large rectangular openings strategically positioned at the maximum shear zone. The primary objective of the experiment was to compare and evaluate various strengthening techniques for these beams. The beams were subjected to two-point loading while supported in a simply supported manner. To establish a basis for comparison, two reference specimens were included: a solid control beam and a control beam with two large openings. The remaining beams were externally strengthened using a range of methods around the openings, including vertical and inclined schemes. Strengthening materials such as GFRP sheets, steel plates, steel bars, epoxy Sikadur 31cf, and GFRP bars with epoxy were utilized. The study focused on investigating parameters of interest, including shear capacity, failure mode, ultimate and first cracking load, crack pattern, ductility, and beam stiffness. The introduction of web openings resulted in a reduction of approximately 59.8% in shear capacity compared to a control solid beam. However, the application of strengthening techniques proved effective in enhancing shear capacity, first crack strength, and load-deflection behavior. The strengthening materials restored shear capacity by 40% to 146% and reduced deflection by 27.5% to 62.5% compared to the reference beam with openings. Ductility increased by 4% to 106%, and stiffness improved by 7% to 97% compared to the control beam with openings. Notably, the inclined reinforcement scheme exhibited greater efficacy in enhancing the load-carrying capability of the beams. Among the various strengthening materials employed, inclined GFRP sheets demonstrated the highest effectiveness and superior performance.

Keywords- Fiber-reinforced concrete; GFRP; shear strengthening; rectangular web opening; near-surface mounted; steel plates; ductility; stiffness.

I. INTRODUCTION

Transversal openings in reinforced concrete beams have gained significant popularity in recent decades due to their numerous advantages. These openings provide flexibility for accommodating building services and facilitate their passage through beams, offering customizable shapes and sizes [1, 2, 3, 4, 5]. Furthermore, they contribute to cost savings by reducing storey heights and self-weight dead loads, while their implementation requires minimal effort. Given the substantial benefits of beams with openings, especially in multi-storey buildings, investigations into their impact on beam performance have become widespread, focusing on critical flexural or shear zones. Openings can be categorized as either large or small. According to Mansour [6], an opening is considered large when its length exceeds the greater depth of the top and bottom chords. For circular openings, it is

recommended to substitute them with an equivalent square. Some and Corley [7] define an opening as large when its depth or diameter exceeds 0.25 times the depth of the beam, and its length exceeds its depth. Previous research has indicated that beams with small openings behave similarly to solid beams and can be analyzed and designed accordingly. However, large openings exhibit distinct behavior and require special consideration in the design process. Numerous analytical and experimental studies have been conducted to assess the impact of large openings on the shear strength of reinforced concrete beams. Abdul-Razzaq and Abdul-Kareem [8] conducted a comprehensive review of previous research studies, investigating the effects of size, shape, location, and the number of openings on the behavior of reinforced concrete T-beams with web and flange openings.

A study conducted by Mohammad Ali and Saeed [9] examined the impact of opening depth, length, and location on the shear strength of reinforced concrete beams. Openings were found to disrupt the formation and angles of struts, causing a deviation in the load path. Additionally, the geometry and slenderness of the beams, represented by the effective length of the chord member divided by its radius of gyration, resulted in a reduction in the compressive capacity of the struts. The ultimate shear strength demonstrated an inverse relationship with the depth and length of the opening. Specifically, an increase in the opening depth from 25% to 40% of the beam depth resulted in a 33% decrease in ultimate shear strength, while an increase in the opening length from 7% to 56% of the shear span led to a 52% decrease. Including top reinforcement in the long chord members is recommended to address bending in beams with openings. Furthermore, openings in beams reduce the cross-sectional area, rendering that particular zone the least resistant to shear stress.

In a study conducted by Elsanadedy et al. [10], two groups of beams were investigated, consisting of un-strengthened and strengthened beams with different opening sizes. The length-to-depth ratio (l_o/h_c) ranged from zero to 6.44 for the un-strengthened beams and 2.0 to 6.44 for the strengthened beams. The authors recommended classifying beams with l_o/h_c less than 1.5 as small openings, as they have minimal influence on the ultimate load and stiffness. Here, l_o represents the length of the opening, while h_c corresponds to the greater depth of either the top or the bottom chord. Beams with l_o/h_c ranging from 1.5 to 4 were categorized as large openings. The reduction in ultimate load and stiffness for un-strengthened beams with l_o/h_c ranging from 1.5 to 4.0 varied



from 23% to 65% and 34% to 69%, respectively. Openings with l_o/h_c exceeding 4.0 were classified as extremely large, as the ultimate load decreased by 71%.

In a study by Jasim et al. [11], ten deep beams were tested, including two solid reference beams and eight beams with large openings in the shear area. The test focused on the variables of opening position and size. Results indicated that as the length of the opening increased from 200 to 230 mm, the first flexural crack, first diagonal crack, and ultimate loads decreased by 14% to 6%, 30% to 8%, and 24% to 9%, respectively. Shifting the openings away from the supports increased the ultimate load by 11%. Furthermore, as the shear span-to-depth ratio increased from 0.9 to 1.1, the ultimate load, first flexural crack load, and first diagonal crack load decreased by 26% to 14%, 23% to 7%, and 20% to 8%, respectively.

In an analysis conducted by Ramadan et al. [12], nine series of beams were examined using the finite element method. The results indicated that openings located near the supports led to a significant reduction of 80% and 82% in cracking and ultimate loads, respectively, compared to beams without openings. For beams with central openings, the reduction reached 40% and 50%, respectively. Furthermore, shallower beams with a span-to-depth ratio of 11.8 exhibited a smaller reduction in cracking and ultimate loads due to the presence of openings, as compared to deeper beams with a span-to-depth ratio of 5.8.

In a comprehensive study conducted by Abdel-Kareem [13], twenty-three reinforced concrete beams with large rectangular web openings at the shear zone were investigated both experimentally and analytically. The study focused on variables such as opening dimensions, location, wrapping amount, type, and configuration. The findings revealed that increasing the opening depth from 33% to 67% of the beam depth resulted in a 58% reduction in ultimate strength. Similarly, increasing the opening length from 19% to 56% of the shear span length decreased the load-carrying capacity by 33%. It was observed that the height of the opening had a more significant impact on the ultimate strength than the beam length. Shifting the beam downward, which decreased the height of the bottom chord from 33% to 17% of the beam height, led to a 27% reduction in ultimate strength. Additionally, shifting the opening towards the support, reducing the distance between the beam and the support from 31% to 12.5% of the shear span length, resulted in a 17% decrease in the ultimate load. These findings indicate that reducing the bottom chord height has a greater influence on the ultimate strength than shifting the opening towards the support.

Extensive research indicates that the presence of large openings significantly impacts the overall behavior of beams. It results in reduced shear and flexural strength, decreased stiffness, increased deflection, and concentrated stresses around the corners of the openings, leading to potential cracking. The introduction of web openings disrupts the normal beam behavior, introducing complexity [14, 15, 5]. When incorporating openings in beams, it's important to reinforce them adequately for structural support. If openings are added later, precautions must be taken to maintain the required strength and stiffness [16, 17]. ACI highlights the

need to consider the impact of openings on shear resistance, especially near supports [18]. Adhering to these guidelines ensures beam stability and performance.

Researchers have extensively studied the strengthening and repair of RC beams with large openings in the shear zone. Various techniques have been proposed, including the use of fiber-reinforced polymer (FRP) sheets and rods for strengthening the openings. Studies conducted by Elansary et al. [19], Abed et al. [20], Rania Salih et al. [21], Elsanadedy et al. [10], Aboul-Nour [22], Maaze and Shoeb [23], and Niea et al. [24] have demonstrated the effectiveness of FRP systems in enhancing shear behavior, improving ductility, and increasing stiffness. In a study by Chin, Shafiq, and Nuruddin [15], six reinforced concrete beams with large openings at the shear zone were examined. The beams were strengthened using CFRP laminates around the openings. The study investigated the openings' dimensions, location, and wrapping details. The results showed a significant increase in beam capacity, approximately 54% when the web openings were strengthened with FRP at a distance from the supports equal to 0.5d or d (beam depth). Additionally, the strengthening led to increased stiffness and reduced cracking and deflection.

In a study by Ahmed et al. [25], the effect of varying steel plate thickness on the reliability of RC beam repair was investigated. The test involved four beams, with one control beam repaired using CFRP and the remaining beams repaired using different thicknesses of steel plates. The findings revealed that RC beams with large openings can be effectively repaired by bonding CFRP sheets or steel plates. Increasing the thickness of the steel plates slightly impacted the load capacity, while CFRP provided a more efficient enhancement of the load capacity compared to steel plates.

Researchers such as Kamonna and ALkhateeb [26], Wiwatrojanagul et al. [27], and Lorenzis et al. [28] have utilized the near-surface mounted (NSM) technique with fiber-reinforced polymer (FRP) rods and steel bars to enhance the shear capacity of reinforced concrete (RC) beams. Their findings demonstrate the practicality of the NSM method in increasing the shear resistance of RC beams.

In a study by Abdel-Kareem et al. [29], thirteen R.C. beams were examined. Steel stirrups were employed to strengthen two beams, while GFRP stirrup rods with different end anchorage and angles were used for eight beams. Two specimens were strengthened using externally bonded GFRP sheets, and one control specimen remained un-strengthened. The findings indicated that beams reinforced with GFRP rods exhibited capacity increases ranging from 14% to 85% compared to the control beam, while beams strengthened with GFRP sheets showed capacity increases ranging from 7% to 22%.

Fiber-reinforced concrete has shown promising results in strengthening structures. Previous studies have highlighted its effectiveness in improving various factors such as corrosion resistance and crack control. Researchers, including Ghahremannejad et al. [30], have explored different aspects of fiber-reinforced concrete, including the type, density, dosage, orientation, and distribution of fibers. This alternative method offers the advantage of replacing conventional internal reinforcement due to its non-corrosive nature and ability to mitigate cracking. Fiber concrete enhances shear,



flexural, and tensile strength while improving ductility and resistance to shrinkage, creep, and impact loading. It effectively reduces crack width and propagation through bridging action, providing high durability and versatility in architectural design [31, 32, 33, 34]. Furthermore, distributed reinforcing in concrete, as emphasized by Marcalikova et al. [34], aims to enhance tensile strength by capturing localized tensile effects resulting from spatial tension between aggregates.

Researchers have extensively investigated the shear behavior of fiber-reinforced concrete beams (Abdul-Zaher et al. [35], Suresh and Prabhavathy [36], Moreno junior and vedoato [37], chalioris and sfiri [38]). Their findings consistently demonstrate that incorporating fibers in the concrete mixture increases the first cracking load, shear capacity, and stiffness while reducing the number and width of cracks. In a study by Ghahremannejad et al. [30], synthetic fiber concrete beams with varying ratios of synthetic fibers and conventional longitudinal reinforcement were tested. The results, obtained using the digital image correlation (DIC) method, indicated that the inclusion of just 1% synthetic fiber enhanced the ultimate load and reduced the number and width of cracks.

II. RESEARCH SIGNIFICANCE

This study investigates the impact of different strengthening materials and configurations on the shear behavior of fiber-reinforced concrete beams with large rectangular openings at the shear zone. GFRP sheets, steel plates, Sika-Dur epoxy, steel bars, and GFRP rods with epoxy are used as external strengthening materials. The study aims to expand knowledge in this area and contribute to future research.

III. EXPERIMENTAL PROGRAM

Eleven specimens were created with uniform dimensions and reinforcement for testing. The specimens had a length of 2200 mm, a rectangular shape with dimensions of 120 mm width and 300 mm depth, and a span of 2000 mm. The concrete cover on all sides was 20 mm thick. The distance between the applied loads was 900 mm. The specimens had an effective depth of 275 mm, resulting in a shear span-to-depth ratio of 2. Shear failure was ensured before any flexural failure. The specimens included four 16 mm deformed bars for tension reinforcement, two 10 mm deformed bars for compression reinforcement, and 8 mm mild steel bars as vertical stirrups spaced at 167 mm intervals.

Refer to Fig. 1 for the dimensions and details of the specimens. Two rectangular openings measuring 110 mm in height and 250 mm in width were introduced at a distance of 275 mm from each support. During the reinforcement fabrication, some stirrups intersected the openings, leading to the cutting of these stirrups. This resulted in U-shaped stirrups at the top and bottom chords of the opening, mimicking openings found in real beams. All specimens were cast using fiber-reinforced

concrete with discrete glass fiber. For further details, refer to Table 1, which provides the test matrix.

The test program consisted of two control specimens: one with openings and one solid specimen without openings. Additionally, nine specimens were strengthened with various materials around the opening, positioned on both sides of the beam. Three layers of GFRP sheets were used to strengthen two beams, steel bars were fixed with steel plates on two beams, GFRP bars using the near-surface mounted technique (NSM) were applied to two beams, and steel plates fixed with steel bolts were used to strengthen two beams. Each group of the eight strengthened specimens had different orientations (vertical and inclined at a 45-degree angle from the longitudinal axis of the beam). The remaining specimen was coated with Sikadur 31CF for external strengthening. The coding system used for the specimens is as follows:

-The two control specimens are labeled as "C" for control.

-The subsequent specimens are labeled based on the type of strengthening material used: "GS" for GFRP sheets strengthening, "SP" for Steel Plate strengthening, "SB" for steel bar strengthening, "GB" for GFRP bar with epoxy strengthening, and "SD" for Sikadur - 31CF strengthening.

-The letters "V" and "I" indicate the orientation of the strengthening, either vertical or inclined at a 45-degree angle.

-The number at the end of the code represents the distance between the bars in mm.

Material Properties:

A. Concrete

The test specimens in this program were specifically made from fiber-reinforced concrete to enhance their shear behavior. Fiber-reinforced concrete consists of the same materials commonly used in ordinary concrete but with the addition of discrete synthetic glass fibers. These fibers were incorporated into the mix at a ratio of 0.8% by volume of the concrete. Table 2 presents the mechanical and physical properties of the discrete synthetic glass fibers as provided by the manufacturer.

For casting the reinforced concrete specimens, high-quality materials were used. This included natural clean siliceous sand, which was free from impurities such as silt, clay, or loam. The sand had a fineness modulus of 2.65 and a specific gravity of 2.6. Crushed dolomite with a maximum aggregate size of 16 mm was utilized, possessing a specific gravity of 2.5 and a fineness modulus of 4.3. Freshwater and discrete glass fiber were also incorporated into the mix.

Furthermore, ordinary Portland cement of grade 42.5N and a superplasticizer called Sika Viscocrete 3425 were added to the mix. The superplasticizer, with a density of 1.08 kg/l, was included in a ratio of 0.8% by weight of the cement. This addition aided in water reduction. The proportions of cement, fine aggregate (sand), and coarse aggregate (crushed dolomite) were combined in a ratio of 1:1.8:3.27, the appropriate amount of water was determined to achieve a water-cement ratio of 0.5, as specified in Table 3, which provides the mixture design.

All the properties of these materials were determined through tests conducted in accordance with standard specifications. The obtained results were compared to the specified limitations outlined in these specifications.

The mixing process involved using a mixer with a capacity of 360 liters, operating at a speed of 50 revolutions per minute.



The sand, fine dolomite, and cement were added to the mixer in a dry state and mixed for three minutes without water. Subsequently, the water and synthetic fiber were introduced, and the entire mixture was further mixed for an additional five minutes to ensure proper blending.

In addition to the beam casts, three cubes with dimensions of 150×150×150 mm were also cast alongside each beam and cured. After 24 hours of casting, the cubes were removed from the molds and submerged in a water tank for a curing period of 28 days. The proportions of the concrete mix were determined through several trial mixes, and the absolute volume method was employed for the concrete mix design.

Compressive Strength: Compression tests were carried out on three cubes measuring 150x150x150 mm for each concrete mix at the age of 28 days in accordance with ASTM C39/C39M-18. The average compressive strength of the fiber-reinforced concrete after 28 days reached 27 MPa.

Tensile Strength: A splitting tensile test was conducted on 28-day cured samples using standard cylinders measuring 150 x 300 mm. The test was performed utilizing a hydraulic testing machine. The average splitting tensile strength observed across all tested specimens was recorded as 2.83 MPa.

B. Steel Bars

Longitudinal reinforcement in the form of deformed steel bars, possessing a yield strength of 400 MPa, was utilized in the construction. The stirrups of all beams were formed using normal mild steel bars with a diameter of 8 mm and a nominal yield strength of 240 MPa. Additionally, all the steel bars employed in the project exhibited a modulus of elasticity measuring 200 GPa.

C. GFRP Sheets

To reinforce the beams around the opening, unidirectional Glass Fiber Reinforced Polymer (GFRP) sheets were employed. The mechanical properties of the GFRP composite material sheets used are provided in Table 4. The attachment of the GFRP sheets to the concrete surface of the tested specimen was accomplished using Sikadur 330, an epoxy resin and adhesive. The mechanical and physical properties of this adhesive are outlined in Table 5.

D. GFRP Bars

Table 6 presents the mechanical properties of the GFRP bars utilized in this study.

E. Sikadur-31CF

Table 7 shows the mechanical and physical properties of the strengthening material Sikadur31CF.

F. Steel Plates

Steel plates of grade ASTM A516, with a thickness of 5 mm, were employed in this study to reinforce the beams around the openings. Sufficient bolts and nuts were utilized, passing through holes, to establish a strong bond between the concrete surface and the steel plates. The supplier-reported properties of the steel plates are as follows: a tensile strength of 370 MPa, a modulus of elasticity of 210 GPa, an elongation minimum of 21, and a yield strength of 240 MPa. The steel plates possess a density of 7850 kg/m³ and a Poisson's ratio of 0.3. Table 8 shows the mechanical properties.

Test Setup: All specimens underwent shear testing using a two-point loading system until failure. The concentrated loads, each equal to P/2, were applied at a distance of 550 mm from both the right and left supports. The testing was conducted at the Reinforced Concrete Laboratory of Benha University Faculty of Engineering, utilizing a testing machine with a maximum capacity of 1000 kN. The load application was facilitated by rigid steel frames supported on a rigid floor, as depicted in Fig. 2.

During the testing process, the hydraulic jack of the testing machine applied the load to the specimen, which was then transferred to the loading points through a steel spreader beam. To ensure the stability and centered positioning of the beam during testing, the test specimen was supported by steel roller bearings that acted on spreader plates, covering the entire width of the beam.

The test specimens were subjected to a simply supported condition with a clear span of 2000 mm. The shear span-to-depth ratio (a/d) was maintained at two, where "a" represents the distance between the applied load and the support. During the experiment, load measurements were obtained using an electrical load cell positioned beneath the hydraulic jack. This load cell was connected to a monitoring system that recorded the applied load values.

To facilitate a detailed observation of crack formation and propagation, the load was incrementally applied to all tested specimens. At each incremental step, the applied load was held constant to visually examine and mark the formation and propagation of cracks on both sides of the beams, as well as to identify failure modes.

For linear displacement measurement, three linear variable differential transformers (LVDTs) were utilized. These LVDTs were placed at the mid-span of the specimen and under the two load points, as shown in Fig. 2. The development and propagation of cracks in each beam were carefully marked, and the modes of failure were recorded for further analysis.

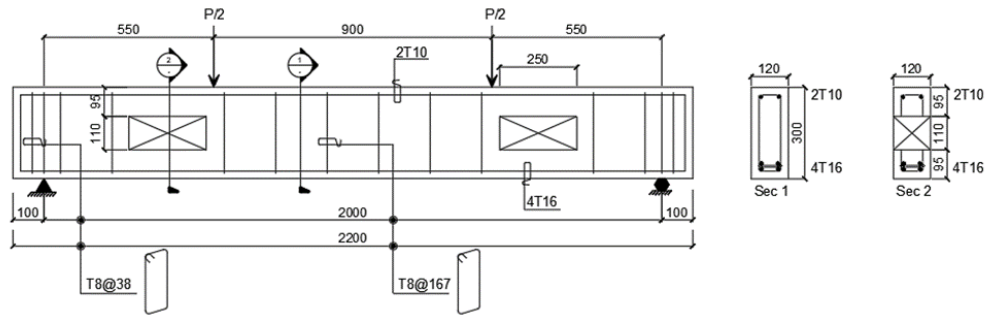
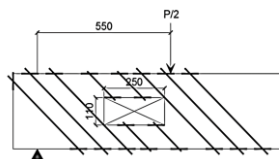
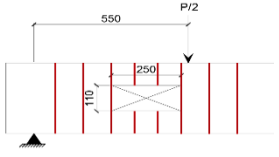
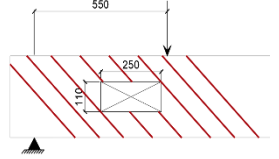
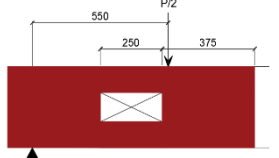


Figure 1. Dimension and reinforcement details of the specimens (Note: all dimensions in mm)

Table 1. Test Matrix

Specimen No.	Beam ID	Strengthening techniques /material	No. of layers	Strengthening configuration	Sketch
1	C-solid beam	-	-	-	
2	C-opening beam	-	-	-	
3	GS-V	EB-GFRP sheets	3		
4	GS-I	EB-GFRP sheets	3	45	
5	SP-V	EB-Steel Plates with bolts	-	90	
6	SP-I	EB-Steel Plates with bolts	-	45	
7	SB-V-100	NSM-Steel links	-	90	

8	SB-I-100	NSM- Steel links	-	45	
9	GB-V-100	NSM-GFRP links with epoxy	-	90	
10	GB-I-100	NSM-GFRP links with epoxy	-	45	
11	SD-V	EBIG-Sikadur - 31CF	1	90	

EB - externally bonded, NSM - near-surface mounted, EBIG- externally bonded in groove.

Table 2. Mechanical / Physical properties of discrete synthetic glass fiber

Property	Value
Ultimate tensile strength	2000 MPa
Young's modulus	5 GPa
Ultimate tensile strain	2.2 %
Density	2.5×10^{-5} N/mm ³
Filament length	24mm \pm 1.5
Filament diameter	15 μ m \pm 2

Table 3. Concrete mixture design

Material	Quantity
Cement	350 kg/m ³
Fine aggregate	630 kg/m ³
Coarse aggregate	1144 kg/m ³
Water reducing admixture	2.8 liter/m ³
W/C	0.5
Vf*	0.8%

* Of the concrete volume.

Table 4. Mechanical properties of GFRP sheets

Property	Value
Length/Roll	5000 mm
Fabric width	500 mm
Design thickness	0.17 mm
Ultimate strength	1480 MPa
Modulus of elasticity	73 GPa
Ultimate elongation	2.8%

Table 5. Mechanical / Physical properties of Sikadur 330 adhesive

Property	Value
Density	1.30 \pm 0.1 kg/l (component A+B mixed) (at +23 °C)
Tensile Strength	30 N/mm ² (7 days at +23°C)
Modulus of Elasticity in Tension	in Flexure: 3 800 N/mm ² (7 days at +23 °C) in Tension: 4500 N/mm ² (7 days at +23 °C)
Elongation at Break	0.9 % (7 days at +23 °C)
Tensile Adhesion Strength	Concrete fracture (> 4 N/mm ²) on sandblasted substrate
Color	Component A: white paste Component B: grey paste Components A + B mixed: light grey paste

Table 6. Mechanical / Physical properties of GFRP bars

Property	Value
Tensile strength	670 N/mm ²
Modulus of elasticity	40000 N/mm ²
Diameter	10 mm
Density	22 kN/m ³

Table 7. Mechanical / Physical properties of Sikadur 31cf adhesive

Property	Value
Density	All types: Comp. (A): 1.65 kg/l Comp. (B): 1.65 kg/l
Tensile strength	Normal/Rapid Type after 10 days at +10-20oC: 15 - 20 N/mm ² L.P Type after 10 days at +20-30oC: 20 - 25 N/mm ²
Modulus of elasticity in tension	4'300 N/mm ² (Static)
Coefficient of thermal expansion	50 x 10 ⁻⁶ per °C (temp. range: -20 °C to +40 °C)



Table 8. Mechanical properties of steel plates

Property	Value
Density	7850 kg/m ³
Tensile strength	370 MPa
Modulus of elasticity	210 GPa
Elongation min, % 200 mm (8 in)	21
Elongation min, % 50 mm (2 in)	25

Applied Strengthening Systems for the Test Specimens:

A. GFRP Sheets Strengthening System

To ensure a robust and secure connection between the GFRP sheets and the concrete surface, several procedures were implemented. The concrete surface was meticulously prepared by thorough washing and cleaning to eliminate any unwanted substances, as depicted in Fig. 3. The GFRP sheets were accurately cut into the required shape to be positioned later around the opening. After the surface treatment, epoxy was applied to all specimens to attach the GFRP sheets. GFRP sheets were placed adjacent to the left and right sides of the opening, following both vertical and skewed orientations of 45 degrees from the longitudinal axis of the beam, as illustrated in Fig. 4. In both orientations, three layers of GFRP sheets were utilized, each with a width of 10 mm. The specimens were air-dried to ensure the elimination of moisture.

For attaching the GFRP sheets to the strengthened area, Sikadur 330 epoxy resin was employed as an adhesive. This adhesive, composed of two components, A and B, was mixed in a weight ratio of 4:1. A thin layer of Sikadur 330 was carefully applied to the concrete surface. A roller tool was

utilized to apply pressure and ensure a firm bond between the GFRP sheets and the concrete surface, thereby eliminating any potential air gaps and removing excess epoxy resin.

B. GFRP Bars Strengthening System

The NSM (Near-Surface Mounted) technique was employed to place GFRP bars around the openings in the specimens. Two separate specimens were strengthened, one with GFRP rods positioned at a 45° angle and the other at a 90° angle. Pre-prepared grooves were formed on the outer surface of the concrete using wooden bars, which were later removed once the concrete had hardened, creating space for the GFRP bars. All grooves had dimensions of 10 mm in depth and 10 mm in width.

To establish a robust connection between the FRP bars and the concrete, thorough cleaning of the grooves was performed, ensuring the removal of any dust or debris. An air-brush compressor was utilized to effectively blow away fine particles and promote a strong bond between the adhesive and the concrete surface. A manual gun was employed to apply the epoxy adhesive paste, partially filling the groove's depth. Subsequently, the GFRP bars were inserted into the grooves and gently pressed to displace the epoxy paste. Additional epoxy was then added to fill any remaining gaps, ensuring that all sides of the GFRP bars were fully covered with epoxy. The surface was leveled and smoothed by removing excess epoxy using a specialized tool.

The specimens were left to allow the epoxy to dry thoroughly before the testing commenced. Detailed information and dimensions of the GFRP strengthening system can be seen in Fig. 5.

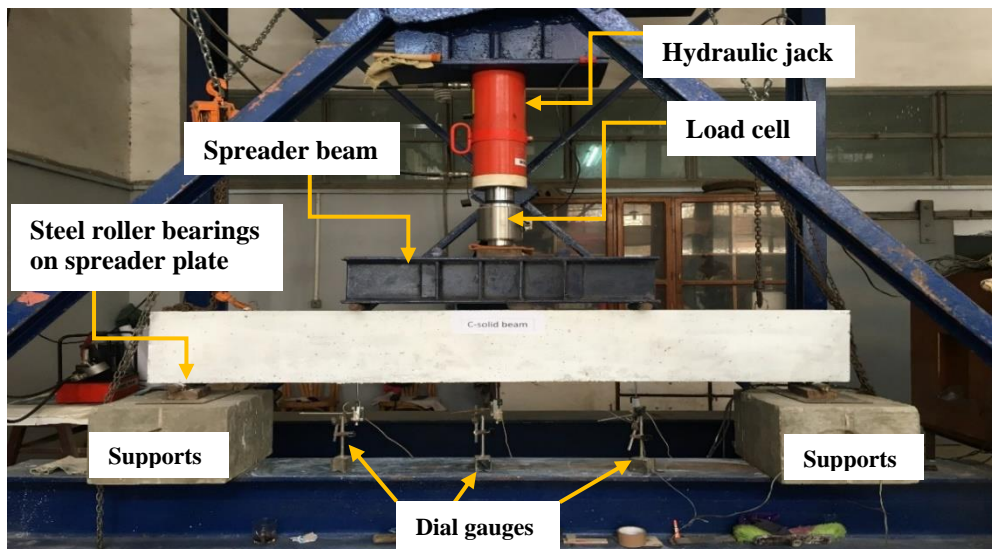


Figure 2. View of the test set-up



(a)

(b)



(c)

Figure 3. Preparing GFRP sheets using epoxy resin

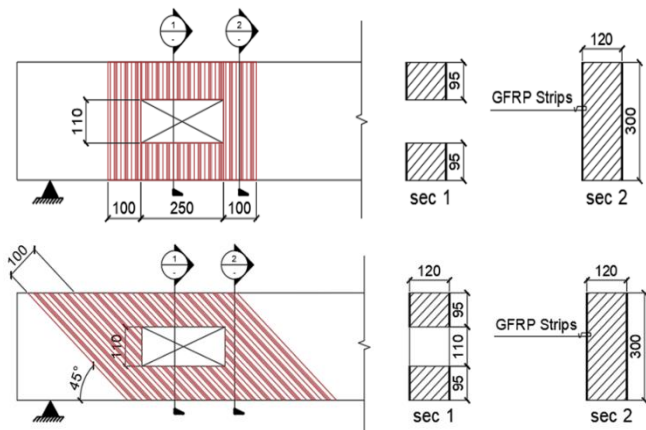
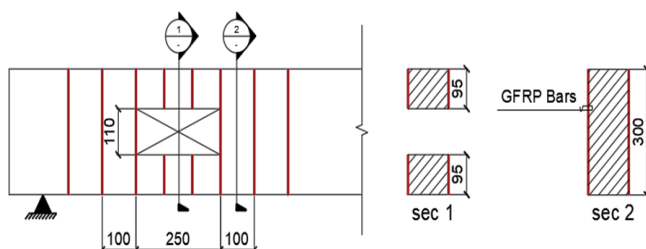


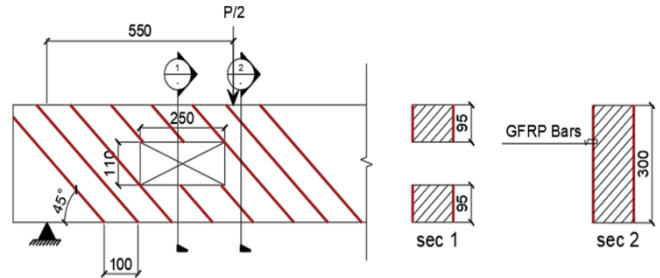
Figure 4. Description of GFRP wrapping configurations around openings



(a) Preparation of Grooves around the opening



(b) Dimensions and details of vertical GFRP links strengthening system



(c) Dimensions and details of horizontal GFRP links strengthening system

Figure 5. GFRP bars strengthening system

C. Steel Plates Strengthening System

To strengthen the specimens using vertical and inclined steel plates, four steel plates with a thickness of 5mm were affixed to the sides of each specimen's cross-section surrounding the openings. These side plates were precisely cut and shaped in vertical and inclined configurations specific to each test specimen.

The concrete surface underwent a thorough washing and cleaning process to eliminate any undesirable substances, ensuring a clean and debris-free surface. Subsequently, the surface was exposed to air, allowing it to completely dry and devoid of any moisture. The steel plates were securely attached to the beam surface using screws, washers, and nuts, as illustrated in Fig. 6a.

For fastening, 10 mm screws were utilized and extended to the opposite side of the beam section through pre-drilled holes made using a drilling machine. The number of screws was carefully selected to ensure sufficient bonding and promote composite action between the specimen surface and the external steel plates. Moreover, circular holes were incorporated into the steel plates at the precise locations of the screws to facilitate proper penetration of each screw.

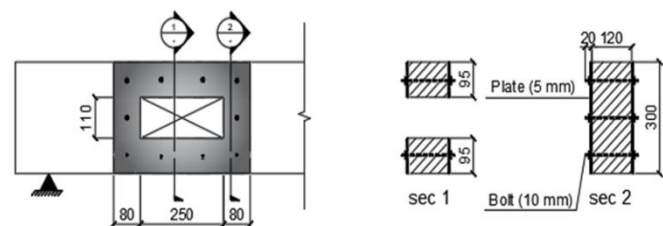
The steel plates were placed within grooves created on the outer surface of the concrete beams, as depicted in Fig. 6b. These grooves had a uniform depth of 10 mm. For further details and dimensions of the steel plates strengthening system, refer to Fig. 6c & d.



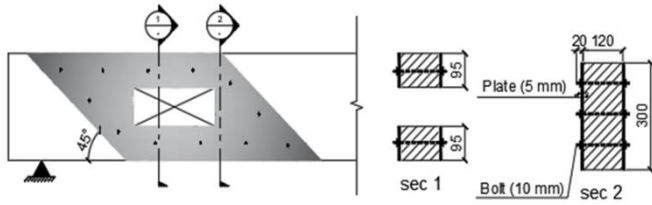
(a)



(b)



(c)



(d)

Figure 6. Steel plates configuration and details

D. Steel links Strengthening System

To reinforce the specimens using steel bars, the steel bars were carefully cut to the required length and securely attached to the beam using steel plates and bolts. Fig. 7 provides a visual representation of this configuration. Pre-prepared grooves were made on the outer surface of the concrete beams to accommodate the steel bars. These grooves had dimensions of 10 mm in depth and 10 mm in width.

The steel bars used had a diameter of 10 mm and were positioned around the openings at regular intervals of 100 mm. For each test specimen, sidebars were shaped and cut accordingly, both in vertical and inclined orientations. At the top and bottom faces of the beam, 10 mm thick steel plates were placed.

To establish a robust connection, two holes were prepared in each steel plate to allow the steel bars to pass through. Subsequently, washers and nuts were employed to secure the steel bars to the beam, ensuring a reliable and sturdy connection.

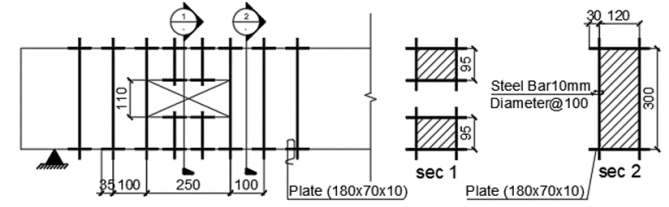
E. Sikadur-31CF Strengthening System

In the specimen strengthened with Sikadur 31CF, meticulous surface preparation was conducted to ensure it was thoroughly cleaned and devoid of any dust or fine particles. Sikadur-31CF is a two-component adhesive consisting of components A and B. These components were meticulously mixed for a minimum of two minutes using a slow-speed electric drill equipped with a mixing paddle. The mixing process continued until the material achieved a smooth consistency and a gray color.

Pre-prepared grooves, as illustrated in Fig. 8a, were created with a depth of 5 mm around the openings. A thin layer of the mixed adhesive was then skillfully applied to the concrete surface using a trowel. The Sikadur-31CF Strengthening System, including specific details and dimensions, can be observed in Fig. 8b.



(a)

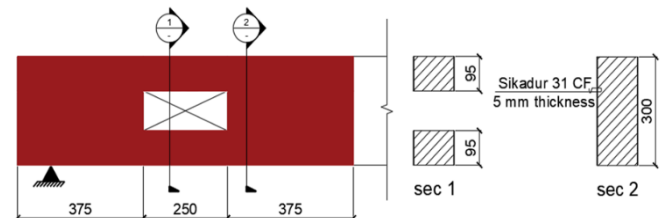


(b)

Figure 7. Steel links fastening system to the concrete beam.



(a)



(b)

Figure 8. Sikadur-31cf strengthening system details and dimensions.

IV. EXPERIMENTAL RESULTS AND DISCUSSIONS

The relationships between the applied loads and the corresponding deflections at mid-span were plotted and first cracking loads and ultimate loads were recorded for all the tested specimens. Results of the test are presented in a summary in Table 9. The maximum load-carrying capacity of the beam, crack patterns and failure modes are discussed in the following sections. Fig. 9 illustrates load-deflection behavior at mid-span for all specimens.

A. Cracking Behavior and Failure Modes

The tested specimens were subjected to shear loading until failure. The initial load at which the first crack appeared was noted for each specimen, and the propagation of cracks was observed and documented at each subsequent load increment to analyze their behavior leading to failure. Fig. 10 provides a visual representation of the structural patterns observed at the



ultimate load for the solid control beam, the control beam with openings, and the vertically strengthened beam using GFRP.

Control Solid Beam: Fig. 11 depicts the crack patterns and failure mode observed in the solid control beam. Initially, thin longitudinal flexural cracks emerged in the tension zone, gradually extending vertically towards the neutral axis of the beam. As the number of flexural cracks increased, they continued to expand, accompanied by the formation of diagonal cracks. Notably, a primary diagonal crack propagated at an angle of approximately 45° relative to the beam's longitudinal axis. The crack width progressively widened, culminating in a sudden brittle shear failure within the shear zone.

Control Beam with openings: In the case of the control beam with openings, the occurrence of cracks was earlier, and the cracks were wider compared to the control beam without openings. Diagonal shear cracks originated from the corners of the openings in the bottom chord, and a diagonal crack formed in the top chord due to stress concentration. Additional secondary cracks were observed in the remaining corners of the opening. The severity of the cracks was greater in the right opening compared to the left opening. Two separate diagonal cracks, situated below and above the opening, initiated from the nearest corner of the opening to the support and load point, forming an angle of approximately 45° . The crack width progressively increased until failure. The failure of the beam exhibited sudden onset of brittle diagonal cracks, with no prior warning. Failure initially occurred in the top chord, followed by the bottom chord. Fig. 12 illustrates the shear failure of the control beam with openings.

Beams with Strengthened Openings: The tested specimens all experienced shear failure at the opening zone. The failure modes observed in the tested beams included the formation of two separate cracks at the top and bottom chords, the development of a primary diagonal shear crack extending from the load point to the support, debonding, or buckling. The failure modes of the specimens with reinforced openings are illustrated in Fig. 13.

In the case of specimens reinforced with GFRP sheets, notable observations were made. The local cracks that initially formed around the openings in the un-strengthened beam transformed into flexural cracks in the beams strengthened with GFRP sheets. This transformation was attributed to the presence of GFRP sheets, which effectively covered the weak area surrounding the openings, resulting in a higher load-carrying capacity compared to the un-strengthened beam with openings. Due to the presence of the GFRP sheets, it was not possible to monitor the propagation of cracks around the openings. However, the first recorded crack for these strengthened beams appeared at the mid-span of the tension zone. As the applied loads increased, both deflection and crack formation intensified, ultimately leading to failure near the point of loading at the top chord of the opening. During failure, local debonding of the GFRP from the concrete surface was observed, and the opening was partially tilted upward, accompanied by localized crushing of the concrete at the top and bottom chords of the opening. Fig. 14 provides a visual representation of the local debonding of the GFRP sheets.

Similar to the specimens strengthened with GFRP sheets, the specimens reinforced with steel plates exhibited a comparable failure mode. The steel plates effectively covered the area surrounding the opening, preventing the development and propagation of cracks in that region and causing them to transform into flexural cracks. Flexural cracks were observed along the tension zone in both the beams with vertical and inclined plates. As the applied load increased, additional cracks formed, and deflection intensified. Ultimately, an abrupt shear failure occurred near the point of loading. This failure led to the upward tilting of the opening, resulting in buckling of the steel plates, followed by crushing of the concrete in the top and bottom chords.

In the specimens reinforced with steel bars, distinct diagonal shear cracks and additional cracks were observed at the corners of the openings. The diagonal shear crack gradually formed from the supports, extending across the steel bars and progressing through the top chord towards the point load. The crack width increased as the load was incremented until failure occurred, accompanied by significant deflections. The angle of the failure crack in the beam with vertical bars was approximately 30° , while in the beam with inclined bars, the angle approached 45° .

In specimens reinforced with GFRP bars, the failure mode was similar to that observed in specimens reinforced with steel bars. Flexural cracks were observed along the tension zone, and as the load increased, the cracks and deflection intensified. Eventually, abrupt cracks formed at the top and bottom chords of the opening, originating from the point of loading. Subsequently, the load decreased despite further incrementation. The angle of the failure cracks in these specimens was approximately 30° .

The specimen strengthened with Sikadur 31-CF exhibited behavior similar to that of the specimens reinforced with GFRP bars. Flexural cracks were observed, and abrupt cracks formed at the top and bottom chords of the opening. However, compared to the control beam with openings, the strengthened specimen demonstrated lower deflection and fewer cracks. The angle of the failure cracks in this specimen was approximately 30° .

Specimens reinforced with GFRP sheets and steel plates exhibited a higher number of cracks, although these cracks had smaller widths in comparison to other reinforced specimens. On the other hand, the specimen strengthened with Sikadur 31-CF showed comparatively less effectiveness when compared to the other strengthening materials utilized in the study.

In the C-solid beam, the maximum observed crack width was 4 mm (0.16 in.), while in the C-opening beam it was 6 mm (0.24 in.), and in the GS-V beam it was 2 mm (0.078 in.). The application of external strengthening enabled the beams to withstand higher loads before the initiation of cracks around the openings, resulting in reduced crack widths. The average spacing between cracks was approximately 70 mm for the C-solid beam, 110 mm for the C-opening beam, and 67 mm for the GS-V beam. The number of flexural cracks decreased in the control beam with openings compared to the control solid beam, and the failure mode exhibited brittleness. The spacing between cracks was greater in the control beam with openings compared to the control solid beam, and the



application of external strengthening further reduced the spacing between cracks.

B. First Cracking and Ultimate Loads

The first cracking load and ultimate load of all specimens were carefully monitored and recorded at each stage of the applied load. Fig. 15 presents a comprehensive comparison of the tested specimens in terms of their first cracking and ultimate loads. The introduction of openings within the shear span had a significant impact on both the first cracking load and failure load.

The control beam with openings experienced a remarkable decrease of 54% in the first cracking load and a 59.8% reduction in the failure load compared to the control solid beam. However, the application of strengthening materials had a notable positive effect on both the first cracking load and the shear strength of the specimens.

The first cracking load exhibited improvements ranging from 28% to 63%, and the ultimate load increased by 40% to 146% when compared to the control beam with openings. Notably, cracks appeared earlier in specimens reinforced with steel bars, whereas specimens strengthened with GFRP bars and vertical steel plates exhibited crack initiation at similar load stages.

Among the strengthening techniques, the specimens reinforced with steel plates and GFRP sheets proved to be more effective in enhancing both the first cracking load and the ultimate load.

The specimens reinforced with inclined schemes exhibited higher ultimate load values compared to the specimens reinforced with vertical schemes. The inclined scheme resulted in a higher ultimate load capacity, ranging from 7.5% to 20% improvement, when compared to the vertical scheme.

C. Ductility Ratio

Ductility plays a crucial role in assessing the ability of structural members to withstand significant inelastic deformations without experiencing a substantial reduction in strength. It also serves as an indicator of potential failure, providing early warning signs. In this study, ductility is defined as the ratio of deflection at the ultimate load to the deflection at the first crack load.

The findings indicate that the presence of two openings in the control specimen greatly impacts the beam, resulting in a 38.7% reduction in ductility compared to the control solid beam. However, the application of shear strengthening materials significantly improves the ductility of the specimens. Notably, the ductility increases by 4% to 106% compared to the control beam with openings.

Among the strengthened specimens, the one reinforced with Sikadur-31CF exhibits the lowest ductility, while the specimens reinforced with GFRP sheets and steel plates demonstrate the highest ductility due to their high modulus of elasticity. Furthermore, it is evident that the use of the inclined

technique results in a significantly higher ductility compared to the vertical technique. Fig. 16 provides a visual comparison of the ductility values for all the strengthened specimens.

D. Stiffness

Stiffness refers to the capacity of elements to resist deformations caused by applied loads, highlighting their rigidity. In this study, the uncracked stiffness (K_i) and ultimate stiffness (K_u) were determined for various specimens based on load and deflection measurements during cracking and ultimate loads. The control beam with openings exhibited a significant decrease of 48.6% in ultimate stiffness compared to the solid control beam. However, incorporating external strengthening materials proved beneficial in enhancing stiffness. Notably, the inclined technique demonstrated the most significant improvement, as the specimen reinforced with inclined GFRP sheets achieved the highest stiffness among all the strengthening materials. Moreover, specimens strengthened with steel plates exhibited symmetrical results similar to those observed with GFRP sheets. The use of external strengthening materials resulted in an increase in initial stiffness ranging from 7% to 97% and an increase in ultimate stiffness ranging from 8% to 50%. On the other hand, the beam strengthened with Sikadur 31CF had a relatively minor effect on stiffness when compared to the other beams. For a visual representation, Fig. 17 provides a comparison of stiffness values for all the strengthened specimens.

E. Energy Absorption Capacity

Energy absorption is a crucial parameter for evaluating the safety and performance of structural elements when subjected to extreme loads and stresses [39]. It represents the ability of these elements to dissipate and withstand energy while carrying loads, providing insights into their brittleness, deterioration, and overall structural capacity [39, 40].

To calculate energy absorption (E), the integral of the deflection-load curve (depicted in Fig. 18) was determined using Simpson's rule (Eq. 1) for all specimens. The results, presented in Table 9, indicate that the presence of openings in the beam significantly reduces energy absorption by approximately 4.93 compared to the control solid beam. However, the strengthened beams exhibit increased energy absorption ranging from 0.77 to 4.94 compared to the control beam with openings. Notably, the inclined technique demonstrates higher energy absorption compared to the vertical technique. Fig. 19, a bar chart, visually illustrates the energy absorption capacity for all the specimens, effectively highlighting the differences among them.

$$A = \frac{P_x + P_{x+1}}{2} (\Delta_{x+1} - \Delta_x) \quad (1)$$

Where: A: Area; P: Load; Δ : Deflection.



Table 9: Summary of test results

Beam ID	P _{cr} (kN)	Diff. of Crack load P _{cr}		P _u (kN)	Diff. of Ult. Load P _u		Δ _{cr} (mm)	Δ _u (mm)	Diff. of Δ _u		Ductility ratio Δ _u /Δ _{cr}	Increase over c-opening in Ductility	un-cracked stiffness (K _i) (kN/mm) P _{cr} /Δ _{cr}	Ult. stiffness (K _u) (kN/mm)		E (kN.mm)	Mode of failure
		P _{cr,c-opening}	P _{cr}		P _{u,c-opening}	P _u			Δ _{u,c-opening}	Δ _u				P _{cr} -P _{cr}	Δ _u -Δ _{cr}		
C-solid beam	80	-----	-----	249	-----	-----	2.20	12.5	-----	-----	5.68	-----	36.36	16.41	3436.56	Flexural shear	
C-opening beam	43	1.00	1.00	100	1.00	1.00	2.30	8.00	1.00	1.00	3.48	1.00	18.70	10.00	579.40	Diagonal shear at the top and the bottom chords	
GS-V	62	1.44	2.05	205	2.05	1.69	2.16	13.5	1.69	1.70	6.25	1.80	28.70	12.61	2982.25	Shear failure + GFRP debonding	
GS-I	70	1.63	2.46	246	2.46	1.70	1.90	13.6	1.70	1.70	7.16	2.06	36.84	15.04	3442.05	Flexural shear + GFRP debonding	
SP-V	60	1.40	1.80	180	1.80	1.41	2.35	11.3	1.41	1.54	4.81	1.38	25.53	13.41	1919.25	Shear failure + steel plate buckling	
SP-I	62	1.44	2.15	215	2.15	1.54	1.84	12.3	1.54	1.35	6.68	1.92	33.70	14.63	2235.13	Shear failure + steel plate buckling	
SB-V-100	55	1.28	1.50	150	1.50	1.25	2.40	10.0	1.25	1.35	4.17	1.20	22.92	12.50	1352.50	Diagonal shear	
SB-I-100	55	1.28	1.63	163	1.63	1.35	2.30	10.8	1.35	1.28	4.70	1.35	23.91	12.71	1431.50	Diagonal shear	
GB-V-100	60	1.40	1.60	160	1.60	1.28	2.35	10.2	1.28	1.36	4.34	1.25	25.53	12.74	1381.00	Diagonal shear	
GB-I-100	60	1.40	1.72	172	1.72	1.36	2.25	10.9	1.36	1.31	4.84	1.39	26.67	12.95	1717.50	Diagonal shear	
SD-V	58	1.35	1.40	140	1.40	1.31	2.90	10.5	1.31	1.04	3.62	1.04	20.00	10.79	1027.35	Diagonal shear at the top and the bottom chords	

Where, P_{cr}: 1st. crack load, P_u: Ultimate load, Δ_{cr}: Deflection at P_{cr} at mid-span, Δ_u: Deflection at 1st. cracking load at mid-span, E: Energy absorption capacity.

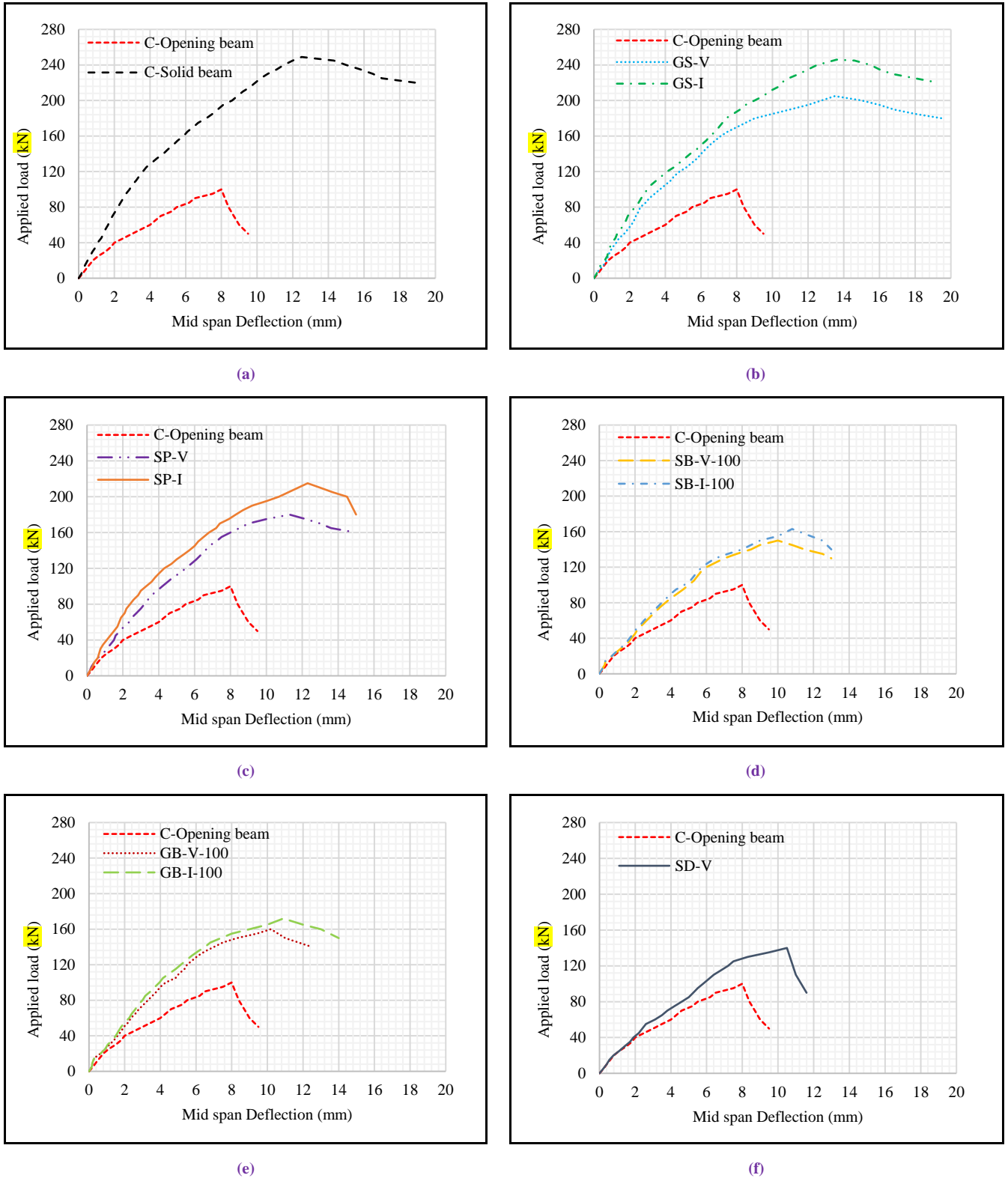


Figure 9. Comparison between load-deflection curves of the specimens

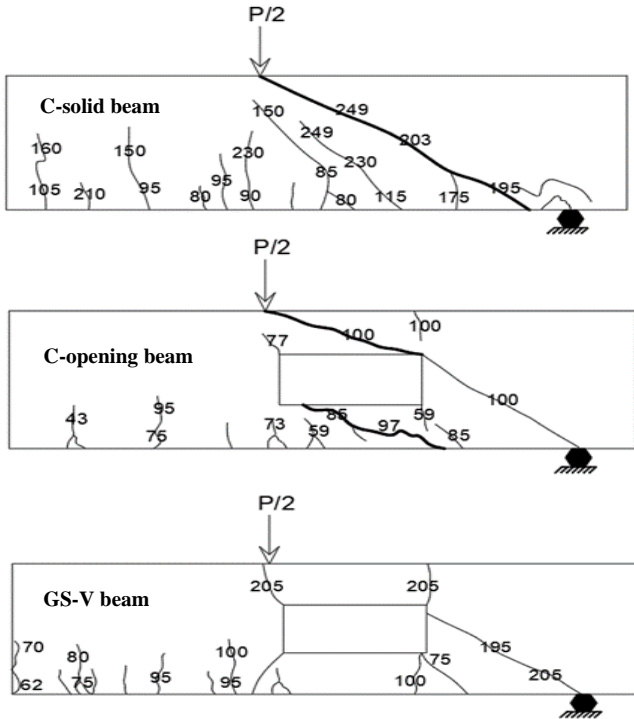


Figure 10. Schematic view of crack pattern at ultimate load for C-solid beam, C-opening beam and GS-V beam.

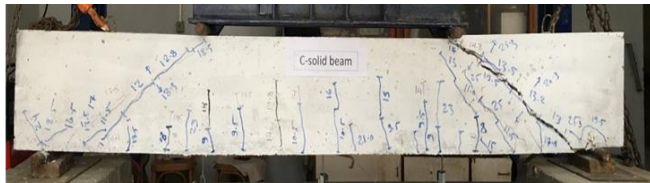


Figure 11. Crack pattern and failure mode of the control solid beam



Figure 12. Crack pattern and failure mode of the control beam with opening



(a) Debonding of GFRP



(b)



(c) Plate buckling



(d)



(e)



(f)



(g)



(h)



(i)

Figure 13. Crack patterns and failure modes of the beams with strengthened openings



Figure 14. Debonding of the GFRP sheets

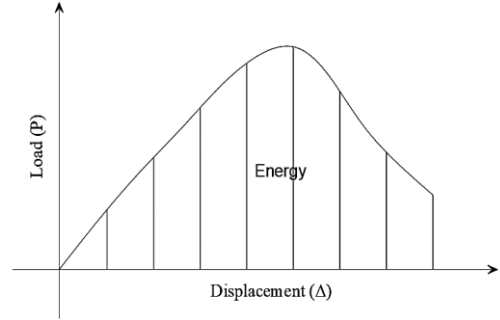


Figure 18. Area Beneath the Load-deflection Curve.

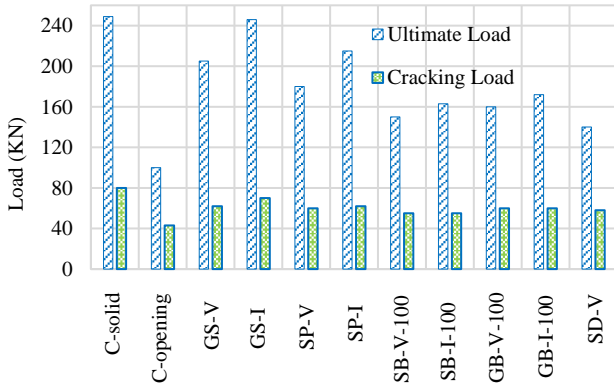


Figure 15. Cracking and ultimate loads comparison

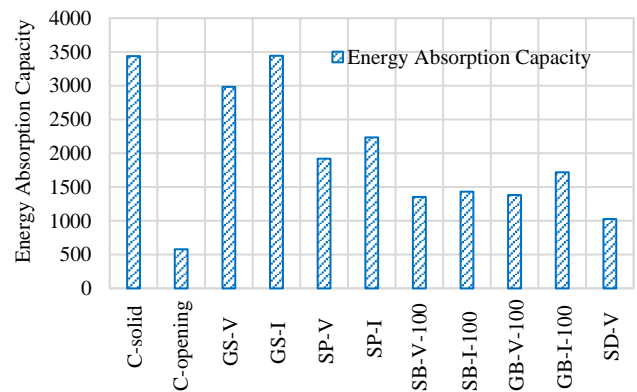


Fig. 19 Obtained Energy Absorption Capacity for Specimens.

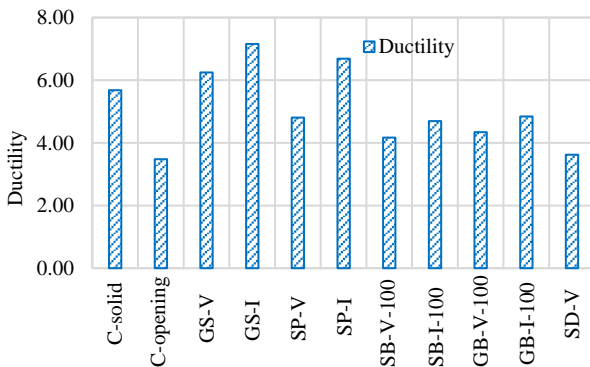


Figure 16. Ductility for Strengthened Specimens

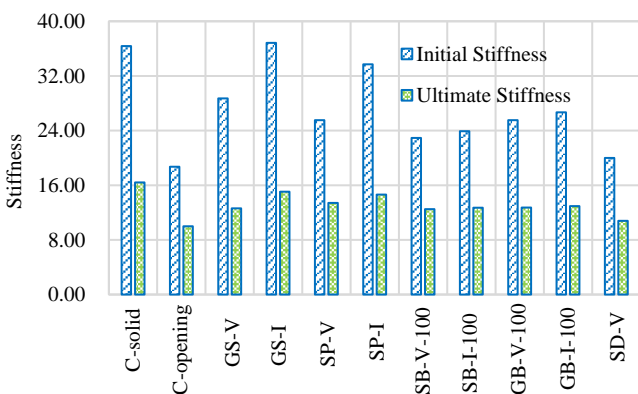


Figure 17. Stiffness for Strengthened Specimens.

V. THEORETICAL STUDY

Table 10 provides a comparison between the shear strength values obtained from the experimental results of this investigation and those predicted by previous research studies as well as the ACI 318 [18] and ACI 440 [41] standards. The purpose of this comparison is to assess the accuracy and reliability of the prediction methods used.

A. Shear Strength Prediction Equation

The shear strength prediction equation for estimating the ultimate shear capacity of a structural element is as follows:

$$V_u = V_c + V_s + V_e \quad (2)$$

Where: V_u : the total shear capacity; V_c : the shear contribution of the glass fiber reinforced concrete; V_s : the shear contribution of the stirrups; V_e : the shear contribution of the external strengthening system.

B. Shear contribution of fiber-reinforced concrete

The shear contribution of fiber-reinforced concrete, V_c , can be calculated using modifications of Zsutty's equation [42] proposed by Ashour et al. [43]. The equation takes into account the influence of fibers and is expressed as:

$$V_c = \left((2.11\sqrt{f'_c} + 7F) \sqrt{\frac{\rho(d-d_o)}{a}} \right) b_w(d-d_o) \quad (3)$$

$$F = \frac{L_f}{D_f} (V_f d_f) \quad (4)$$

Where: F : the fiber factor; ρ : tension reinforcement ratio; a : shear span; b_w : width of the web; d : effective depth of the beam; L_f : fiber length, mm; D_f : fiber diameter, mm; V_f : percentage of fibers by volume; d_o = depth of the opening; d_f : factor represents different bond characteristics of fibers (0.5 for round section fibers, 0.75 for crimped fibers, and 1 for deformed end fibers), 0.75 for crimped fibers, 1 for deformed end fibers. In this research 0.5 was used. For the rectangular cross-section glass fiber, the proportional equation of fiber diameter was

$$D_f = \sqrt{\frac{4t_f w_f}{\pi}} \quad (5)$$

Where: t_f : fiber sheets thickness; w_f : fiber sheets width

C. Shear contribution of stirrups

M.A. Mansur (2006) reported that the vertical reinforcement that can resist shear are the stirrups by the opening sides across a distance equal to $(d_v - d_o)$. The shear contribution of stirrups, V_s , can be expressed as:

$$V_s = \frac{A_v f_y}{s} (d_v - d_o) \quad (6)$$

Where: V_s : shear contribution of stirrups; d_v : the distance between the top and bottom longitudinal rebars, d_o : The diameter or the depth of the opening, A_v : area of vertical legs of stirrups per spacing s ; f_y : yield stress of stirrups.

D. Shear contribution of external strengthening material

Shear contribution of GFRP sheets and bars:

ACI 440 [41] proposed equation that can be used to calculate the shear capacity of GFRC-enhanced beams. The shear resistance of the GFRP sheets and bars is then given by

$$V_f = \frac{A_f f_{fe} d_f (\sin \alpha_f + \cos \alpha_f)}{S_f} \quad (7)$$

Where: A_f is the area of external fiber reinforcement, f_{fe} is the effective stress for fiber at failure, d_f is the effective depth of the FRP, S_f is the spacing between GFRP sheets or bars, α_f : The angle between the fiber and the beam's axis.

Shear contribution of steel plates:

According to Barnes et al. [44] the shear contribution of steel plates can be expressed using the following equation

$$V_p = \frac{1}{3} K f_{yp} h_p t_p \quad (8)$$

$$K = 0.68 - 0.27\rho_v + 0.28\left(\frac{h_p}{h}\right) - 1.95\left(\frac{t_p}{b_w}\right) - 0.007\left(\frac{f_{yp}}{f'_c}\right) \quad (9)$$

Where: ρ_v is the shear reinforcement ratio, h_p is the height of the steel plates, h is the height of the beam, t_p is the steel plate's thickness, f_{yp} is the steel plate yield stress.

Shear contribution of steel bars:

The shear capacity equation proposed by ACI 318 [18] can be used to estimate the steel bars' shear resistance. The shear resistance of the steel bars is then given by

$$V_s = \frac{A_s f_y d_s (\sin \alpha_s + \cos \alpha_s)}{S_s} \quad (10)$$

Where: A_s is the area of external steel bars, f_y is the yield stress for steel bars, d_s is the total height of the steel bars, S_s is the spacing between the steel bars, α_s : The inclination of steel bars relative to longitudinal axis of the beam.

Shear contribution of Sikadur 31CF epoxy:

The shear capacity equation proposed by ACI 440 [41] can be used to estimate the shear resistance of the epoxy Sikadur 31cf is then given by

$$V_r = \frac{A_r f_{yr} d_r}{L} \quad (11)$$

Where: A_r is the area of the epoxy, f_{yr} is the yield stress for the epoxy, d_r is the effective depth of the epoxy as shown in Fig. 20, L is the length of the epoxy layer, h is the beam height.

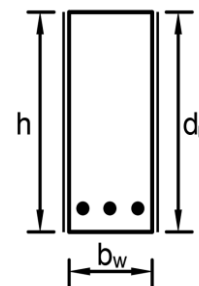


Figure 20. Illustration of the effective depth of the strengthening material

Table 10 presents a comparative analysis between the experimental shear force $V_{u(\text{exp})}$ and the predicted shear force $V_{u(\text{pred})}$ for the strengthened specimens. The ratio (k) calculated as the ratio of $V_{u(\text{exp})}$ to $V_{u(\text{pred})}$, is also provided to assess the accuracy of the predictions. Furthermore, Fig. 21 visually represents the experimental and analytical shear forces of the strengthened specimens through a bar chart.



Previous research studies have demonstrated that the proposed equations exhibit satisfactory accuracy in estimating the contribution of strengthening materials to shear in glass fiber reinforced concrete beams with openings. These findings validate the effectiveness of the analytical predictions in assessing the shear resistance of such strengthened beams.

VI. COST ANALYSIS STUDY

A comprehensive cost analysis study was conducted to evaluate the economic feasibility of the various strengthening materials and configurations employed in this research. The objective was to identify the most cost-effective technique for enhancing the shear capacity of beams with openings. The cost study included, the cost of the strengthening materials, The labor cost of the installation and application of the strengthening materials, such as cutting, grooving, bonding, and curing.

The findings of the cost analysis revealed that the use of steel plates yielded the highest capacity gain per unit cost among the different strengthening techniques. GFRP sheets also demonstrated favorable results in terms of cost-effectiveness. The utilization of GFRP and steel bars exhibited comparable outcomes. On the other hand, the Sikadur 31cf epoxy material was found to be less effective; however, it required relatively less time and effort for preparation. Notably, the process of drilling holes in the steel plates for screw placement and passage through the beam, as required for beams strengthened with steel plates, demanded more time and precision compared to other methods. Similarly, in the case of steel bar reinforcement, meticulous drilling of steel plates was crucial to ensure proper connection and functionality of the bars. The distinction in results between the vertical and inclined schemes was not significant.

A visual representation in the form of a comparative chart in Fig. 22 illustrates the gain in capacity per unit material cost for all the strengthened specimens. This information aids in making informed decisions regarding the selection of the most cost-effective strengthening technique for beams with openings subjected to shear loading.

Table 10. the experimental and analytical shear force results

Beam ID	experimental	predicted	$K = \frac{V_{u \text{ exp}}}{V_{u \text{ pred}}}$
	$V_{u \text{ exp}}$ (kN)	$V_{u \text{ pred}}$ (kN)	
C-solid beam	124.5	123.99	1.00
C-opening beam	50	60.83	0.82
GS-V	102.5	100.43	1.02
GS-I	123	116.83	1.05
SP-V	90	114.03	0.79
SP-I	107.5	135.33	0.79

SB-V-100	75	96.63	0.78
SB-I-100	81.5	110.83	0.74
GB-V-100	80	96.63	0.83
GB-I-100	86	110.95	0.78
SD-V	70	77.13	0.91

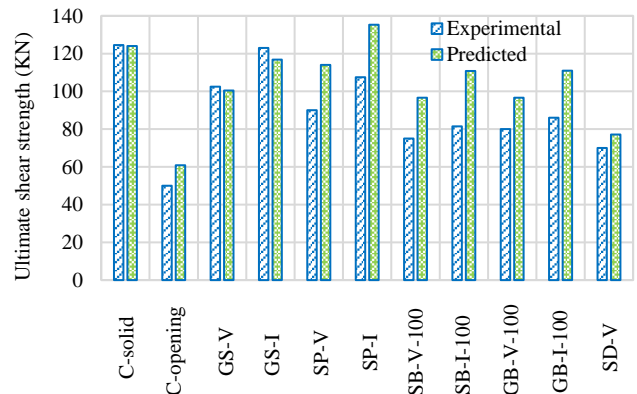


Figure 21. Comparison between the experimental and predicted ultimate shear strength.

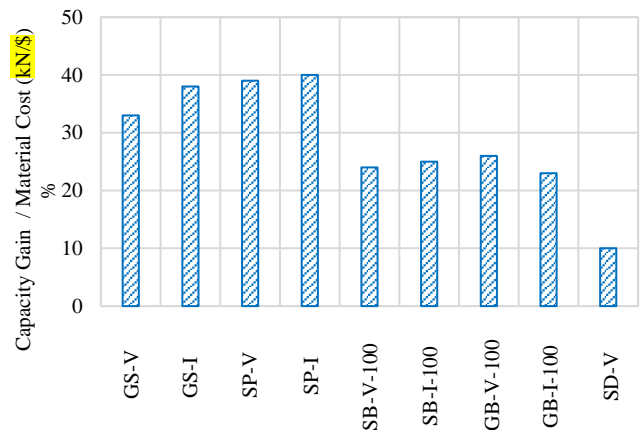


Figure 22. Percentage of capacity gain per material cost for strengthened specimens.

VII. CONCLUSION

In conclusion, the experimental analysis conducted in this study provided valuable insights and comparisons regarding the behavior of beams with web openings and the effectiveness of various strengthening techniques. The key findings are as follows:

- The presence of large web openings in the shear zone of beams resulted in a significant reduction in shear capacity and stiffness, with a reduction of approximately 59.8% in shear capacity observed.
- Shear failure in all tested beams was characterized by diagonal shear cracks between the strengthening



material surrounding the openings, the loading point, and the support.

- The strengthened beams exhibited a reduction in secondary cracks along the tension zone compared to the un-strengthened control beam, and they demonstrated lower deflections at the same loading level as the control beam with openings.
- Strengthening with steel bars around the openings increased the first cracking load by 28% compared to the control beam with openings, and it improved the ultimate load by approximately 50% to 63%.
- The near-surface mounted (NSM) technique using glass fiber reinforced polymer (GFRP) bars proved to be highly effective in increasing the shear capacity of reinforced concrete (RC) beams. In this study, a significant improvement of 72% in shear capacity was achieved compared to the control beam with openings.
- The effectiveness of shear strengthening materials was found to be influenced by the inclination of their placement. Beams strengthened with vertical shear strengthening materials restored 40% to 105% of the shear capacity of the control beam with openings, while inclined shear strengthening materials restored 72% to 146% of the shear capacity of the control beam with openings.
- The creation of openings in beams resulted in a considerable reduction in ductility. However, the use of external strengthening materials effectively restored and even enhanced the ductility of the beams. Notably, GFRP sheets proved to be highly effective, with beams strengthened with inclined GFRP sheets exhibiting a ductility increase of 106% compared to the control beam with openings.
- The stiffness of the beams was significantly affected by the presence of web openings, with initial and ultimate stiffness reduced by 48.6% and 93.9%, respectively, compared to the control solid beam. However, the application of external strengthening materials led to an increase in initial and ultimate stiffness by approximately 97% and 50%, respectively.
- Creating web openings resulted in a substantial decrease in the energy absorption capacity of the beams, with a reduction of approximately 4.93 compared to the control solid beam. However, the proposed strengthening techniques proved to be effective in resisting the size effect of openings and restoring the energy absorption capacity.

VIII. RECOMMENDATIONS

Based on the findings of this research, the following recommendations are proposed for future research:

- Investigate different shear span-to-depth ratios to determine their effect on the strength of fiber-reinforced concrete beams with openings.
- Investigate the size effect due to fracture in RC beams failing in shear, to better understand how

experimental results at the laboratory scale can be transferred to engineering practice.

- Examine the effect of various amounts and types of internal reinforcement on the strength of fiber-reinforced concrete beams with openings.
- Investigate the effect of varying the strength of concrete and using different fiber types and ratios on the strength of fiber-reinforced concrete beams with openings.
- Future research should tackle the challenges of applying laboratory-scale results to engineering practice by creating scaling laws for fracture-induced size effect in RC beams with shear failure.
- Investigate the influence of other factors that may affect the strength of fiber-reinforced concrete beams with openings, such as the location and size of the openings, the type and amount of fibers used, and the age of the concrete.
- In addition, future studies should consider using advanced testing techniques, such as digital image correlation and acoustic emission monitoring, to better understand the crack propagation and failure mechanisms in fiber-reinforced concrete beams with openings.
- Finally, efforts should be made to disseminate the research results to the engineering community, through publications, presentations, and collaborations with industry partners, to ensure that the findings are incorporated into the design and construction practices of fiber-reinforced concrete structures with openings.

Funding: This research has not been conducted under any fund.

Conflicts of Interest: The authors declare that there is no conflict of interest.

REFERENCES

- [1] Ahmed M. Sayed (2019), "Numerical study using FE simulation on rectangular RC beams with vertical circular web openings in the shear zones", *Engineering Structures*, **198**.
- [2] Waleed El-Demerdash (2013), "Design of reinforced concrete beams with openings", Ms.D. Dissertation, Mansoura University, Mansoura.
- [3] Tamer el-maaddawy and Bilal el-ariss (2012), "Behavior of concrete beams with short shear span and web opening strengthened in shear with CFRP composites", *Journal of Composites for Construction*, **16**(1).
- [4] PCA (2008), "Notes on ACI 318-08 Building Code Requirements for Structural Concrete", *Portland Cement Association*, United States.
- [5] M.A. Mansur (2006), "Design of reinforced concrete beams with web openings", *Proceedings of the 6th Asia Pacific Structural Engineering and Construction Conference (APSEC 2006)*, Kuala Lumpur, Malaysia.
- [6] M.A Mansur (1998), "Effect of openings on the behavior and strength of R/C beams in shear", *Cement and Concrete Composites*, **20**, 477-486.
- [7] N.F. Somes and W.G. Corley (1974), "Circular openings in webs of continuous beams", *American Concrete Institute*, 359-398.
- [8] Khattab Saleem Abdul-Razzaq, Mais Malallah Abdul-Kareem (2017), "Behavior of RC T-Beams with Openings - Literature Review", *The Second Conference of Post Graduate Researches*, Baghdad, Iraq, October.
- [9] Sardar R. Mohammad Ali and Jalal A. Saeed (2022), "Shear capacity and behavior of high-strength concrete beams with openings", *Engineering Structures*, **264**.
- [10] Hussein M. Elsanadedy, Yousef A. Al-Salloum, Tarek H. Almusallam, Abdulhafiz O. Alshenawy, Husain Abbas (2019), "Experimental and



- numerical study on FRP-upgraded RC beams with large rectangular web openings in shear zones”, *Construction and Building Materials*, **194**, 322–343.
- [11] Waleed A. Jasim, Abbas A. Allawi, Nazar K. Oukaili (2018), “Strength and serviceability of reinforced concrete deep beams with large web openings created in shear spans”, *Civil Engineering Journal*, **4**(11), 2560-2574.
- [12] Osman M. Ramadan, Kamal G. Metwally, and Wafaa M. Shaban (2015), “Proposed recommendations for the design of reinforced concrete beams with openings”, *Advances in Structural Engineering and Mechanics*, 2015 world congress, Incheon, Korea.
- [13] Ahmed H. Abdel-Kareem (2014), “Shear strengthening of reinforced concrete beams with rectangular web openings by FRP Composites”, *Advances in Concrete Construction*, **2**(4), 281-300.
- [14] Ahmed S. Hamzah and Ammar Y. Ali (2020), “Shear behavior of reinforced concrete beams with vertical and transverse openings”, *Test engineering & management*, **83**, 22120-22133.
- [15] S.C. Chin, N. Shafiq and M.F. Nuruddin (2012), “Strengthening of RC beams with large openings in shear by CFRP laminates: experiment and 2D nonlinear finite element analysis”, *Research Journal of Applied Sciences, Engineering and Technology*, **4**(9), 1172-1180.
- [16] Ceyhun Aksoylu, Sakir Yazman, Yasin Onuralp Özkılıç Lokman Gemi, Musa Hakan Arslan (2020), “Experimental analysis of reinforced concrete shear deficient beams with circular web openings strengthened by CFRP composite”, *Composite Structures*, **249**.
- [17] C.-C. Chen, C.-Y. Li and M.-C. Kuo (2008), “Experimental study of steel reinforced concrete beams with web openings”, *The 14th World Conference on Earthquake Engineering*, Beijing, China, October.
- [18] ACI Committee 318 (2014), “Building code requirements for structural concrete (ACI 318-14) and commentary”, *American Concrete Institute*, Farmington Hills, MI 48331.
- [19] Ahmed A. Elansary, Aya A. Abdel Aty, Hany A. Abdalla, Mohamed Zawam (2022), “Shear behavior of reinforced concrete beams with web opening near supports”, *Structures*, **37**, 1033-1041.
- [20] Mohammed J. Abed, Moatasem M. Fayyadh, Omar R. Khaleel (2021), “Effect of web opening diameter on performance and failure mode of CFRP repaired RC beams”, *Materials Today: Proceedings*, **42**, 388-398.
- [21] Rania Salih, Fangyuan Zhou, Nadeem Abbas and Aamir Khan Mastoi (2020), “Experimental Investigation of Reinforced Concrete Beam with Openings Strengthened Using FRP Sheets under Cyclic Load”, *Materials*, **13**.
- [22] Louay A. Aboul-Nour, Mahmoud A. Khater, Magdy K. Khamis and Marwa A. Ibrahim (2018), “Openings in RC Beams and Assessing CFRP Strengthening”, *International Journal of Trend in Research and Development*, **5**(6), 2394-9333.
- [23] Mohammed Rihan Maaze, Mudassir Shoeb (2018), “Strengthening and rehabilitation of RC beams with openings using CFRP”, *i-manager’s Journal on Civil Engineering*, **8**(1).
- [24] X.F. Niew, S.S. Zhang, J.G. Tenga, G.M. Chenc (2018), “Experimental study on RC T-section beams with an FRP-strengthened web opening”, *Composite Structures*, **185**, 273–285.
- [25] A. Ahmed A, S. Naganathan, K. Nasharuddin, M.M. Fayyadh (2015), “Repair effectiveness of CFRP and steel plates in RC beams with web opening: effect of plate thickness”, *International Journal of Civil Engineering*, **13**(2), 234-244.
- [26] Hayder H. kamonna, Lubna R. alkhateeb (2020), “Strengthening of reinforced concrete deep beams with openings by near surface mounted steel bar”, *Journal of engineering science and technology*, **15**(4), 2559-2579.
- [27] Pongsak Wiwatrojnanagul, Borvorn Israngkura Na Ayudhya and Raktipong Sahamitmongkol (2012), “NSM FRP shear strengthening of RC beams with internal stirrups”, *Thammasat International Journal of Science and Technology*, **17**(1), 16-30.
- [28] Laura De Lorenzis and Antonio Nanni (2001), “Shear Strengthening of Reinforced Concrete Beams with Near-Surface Mounted Fiber-Reinforced Polymer Rods”, *ACI Structural Journal*, **98**(1), 60-68.
- [29] Ahmed H. Abdel-kareem, Ahmed S. Debaiky, Mohamed H. Makhlof and M. Abdel-baset (2021), “Shear strengthening of reinforced concrete beams using NSM/EBR techniques”, *Advances in Concrete Construction*, **12**(1), 63-74.
- [30] Masoud Ghahremannejad, Maziar Mahdavi, Arash Emami Saleh, Sina Abhaee, Ali Abolmaali (2018), “Experimental investigation and identification of single and multiple cracks in synthetic fiber concrete beams”, *Case Studies in Construction Materials*, **9**.
- [31] Kiran Kumar Poloju, Chiranjeevi Rahul and Vineetha Anil (2018), “Glass fiber reinforced concrete (GFRC) - strength and stress strain behavior for different grades of concrete”, *International Journal of Engineering & Technology*, **7**(4.5), 707 – 712.
- [32] Praveen Kumar Goud.E and Praveen K.S (2011), “Optimization of percentages of steel and glass fiber reinforced concrete”, *International Journal of Research in Engineering and Technology*, **4**(4), 2321 – 7308.
- [33] Shoeib Soliman Ata Elkareim and Osman Moustaf (2011), “Experimental analysis of R.C. beam strengthened with discrete glass fiber”, *Architecture and Civil Engineering*, **9**(2), 205 – 215.
- [34] Zuzana Marcalikova, Miroslav Racek, Pavlina Mateckova, Radim Cajka (2020), “Comparison of tensile strength fiber reinforced concrete with different types of fibers”, *Procedia Structural Integrity*, **28**, 950 – 956.
- [35] Ahmad Saudi Abdul-Zaher, Laila Mahmoud Abdul-Hafez, Yasser Rifat Tawfic, Osama Hamed (2016), “Shear behavior of fiber reinforced concrete beams”, *Journal of Engineering Sciences*, **44**(2), 132 – 144.
- [36] J.Suresh, R. Angeline Prabhavathy (2014), “Behaviour of Steel Fibre Reinforced Concrete Beams with Duct Openings Strengthened by Steel Plates”, *International Journal of Advanced Information Science and Technology*, **28**(28), 2319-2682.
- [37] A. L. moreno junior and A. P. vedoato (2011), “The shear strength of steel fiber-reinforced concrete beams”, *Ibracon Structures and Materials Journal*, **4**(5), 784-791.
- [38] C. E. chalioris, E. F. sfiri (2011), “Shear Performance of Steel Fibrous Concrete Beams”, *Procedia Engineering*, **14**, 2064–2068.
- [39] S. Mohsenzadeh, A. Maleki, M. A. Lotfollahi-Yaghinb (2019), “Experimental and numerical study of energy absorption capacity of glass reinforced self-compacting concrete beams”, *International Journal of Engineering*, **32**(12), 1733-1744.
- [40] Dr. M. TamilSelvi, D. Yuvaraj, Dr. A. K. Dasarathy, S. Ponkumarelango and R. Subalakshmi (2017), “Assessment of energy absorption of steel, polypropylene and hybrid fiber reinforced concrete prisms using-graph software”, *International Journal of Civil Engineering and Technology*, **8**(10), 1269–1276.
- [41] ACI Committee 440 (2008), “Guide for the Design and Construction of Externally Bonded FRP Systems for Strengthening Concrete Structures”, (ACI 440.2R-02), *American Concrete Institute*, Farmington Hills, Mich.
- [42] Dinh, H.H., Parra-Montesinos, G.J. and Wight, J.K. (2011), “Shear strength model for steel fiber reinforced concrete beams without stirrup reinforcement”, *J. Struct. Eng.*, **137**(10), 1039- 1051.
- [43] Ashour SA, Hasanain GS and Wafa FF (1992), “Behaviour of high-strength fiber reinforced concrete beams”, *ACI Structural Journal*, **89**(1), 176–184.
- [44] Richard Andrew Barnes, Geoffrey Charles Mays (2006), “Strengthening of reinforced concrete beams in shear by the use of externally bonded steel plates: Part 1- Experimental programme”, *Construction and Building Materials*, **20** (2006), 396–402.